Progress In Electromagnetics Research, Vol. 118, 151–165, 2011

ANALYSIS OF DEPENDENCE OF RESONANT TUNNELING ON STATIC POSITIVE PARAMETERS IN A SINGLE-NEGATIVE BILAYER

W.-H. Lin[1], C.-J. Wu[2,*], T.-J. Yang[3], and S.-J. Chang[1]

[1]Institute of Microelectronics, Department of Electrical Engineering, Center for Micro/Nano Science and Technology and Advanced Optoelectronic Technology Center, National Cheng Kung University, Tainan 70101, Taiwan, R.O.C.

[2]Institute of Electro-Optical Science and Technology, National Taiwan Normal University, Taipei 11677, Taiwan, R.O.C.

[3]Department of Electrical Engineering, Chung Hua University, Hsinchu 30012, Taiwan, R.O.C.

Abstract—It is known that electromagnetic resonant tunneling phenomenon can be found in the single-negative (SNG) bilayer, a two-layer coating made of the epsilon-negative (ENG) and the mu-negative (MNG) media. In this work, we report that this resonant tunneling is strongly dependent on the static positive parameters in SNG materials. The values of the static permeability in ENG layer and the static permittivity in MNG layer for obtaining the resonant tunneling are theoretically analyzed and discussed for two possible cases of equal- and unequal-thicknesses. Useful design guidelines in selecting positive parameters for the resonant tunneling are obtained. We also investigate the possible influence in the resonant tunneling due to the losses from the ENG and MNG materials. Additionally, we examine the polarization-dependent resonant tunneling, that is, the dependence of angle of incidence is examined.

1. INTRODUCTION

Electromagnetic metamaterials (MTMs) with simultaneously negative real parts of the complex permittivity and the complex permeability have attracted much attention over the past decade. The idea of

Received 2 April 2011, Accepted 22 June 2011, Scheduled 30 June 2011

* Corresponding author: Chien-Jang Wu (jasperwu@ntnu.edu.tw).

MTMs was first suggested early in 1968 by Veselogo who considered a lossless MTM and showed that in such a medium the Poynting vector is antiparallel to the wave vector [1]. Today, the existence of simultaneously negative real permittivity and permeability in a medium leads to the definition of double-negative (DNG) medium. The antiparallel property, in turn, gives rise to another familiar name for this medium, the left-handed medium (LHM), since in this medium the electric field, the magnetic field, and the wave vector follow a left-handed triad. It was until in 2000 that the idea of Veselago was experimentally realized in the microwave regime by Smith et al., who constructed an artificial composite medium consisting of arrays of metallic thin wires (TWs) and split ring resonators (SRRs) [2, 3]. There have been many reports on the electromagnetic and optical properties for the structures containing DNG metamaterials [4–13].

The array of metallic TWs constitutes another type of MTMs, i.e., it is a medium with a negative real part of complex permittivity but with a positive real permeability. This is called an epsilon-negative (ENG) medium. Similarly, the array of SRRs leads to a medium with a negative real part of complex permeability but with a positive real permittivity, which is known as a mu-negative (MNG) medium. Both ENG and MNG media are now referred to as the single-negative (SNG) media. With this single-negative feature, the wave number will be complex-valued, i.e., it has an imaginary part. As a result, a wave in an SNG medium will be evanescent and thus it cannot propagate in the medium. Nevertheless, like the DNG media, the SNG media also exhibit some unusual electromagnetic wave features. By pairing the SNG media in a conjugate manner, Fredkin and Ron have shown that such a combination may effectively act as an LHM because the effective group velocity is antiparallel to the phase velocity [14]. In a one-dimensional SNG photonic crystal (PC), that is formed by repeating the ENG-MNG bilayers, there is an SNG gap which exhibits some salient features different from the Bragg gap in a usual photonic crystal [15–18]. This new SNG gap also called zero-effective-phase gap stems from the interactions of the forward and backward evanescent waves in the SNG layers. Layered structures containing SNG materials have attracted much attention in recent years [19–31].

In a basic structure of ENG-MNG bilayer depicted in Fig. 1, we assume that the regions 0 and 3 are the same media as free spaces. In this conjugated configuration, Alu and Engheta have pointed out some interesting wave characteristics, such as resonance, complete tunneling and transparency [19]. Recently, Ding et al. have reported that the resonant tunneling phenomenon can also be found in a nonconjugated ENG-MNG bilayer [20]. Electromagnetic tunneling problem has been

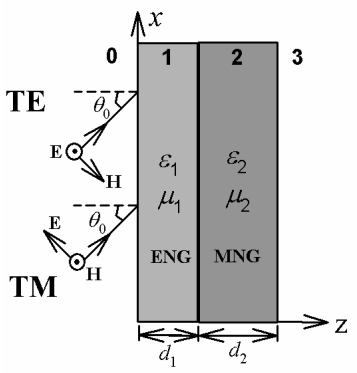

Figure 1. An SNG bilayer structure, in which the constituent ENG layer (region 1) and MNG layer (region 2) have thicknesses of d_1 and d_2, respectively. A wave is incident obliquely on the plane boundary of $z = 0$. Two possible polarizations, TE and TM waves, are shown. The incident angle is denoted by θ_0.

extended to a trilayer structure containing SNG metamaterials [21–23]. In reference [21], resonant tunneling has been found in a structure of MNG-Air-ENG. A three-layer structure, SNG-DPS-DPS (DPS means the double-positive medium), is investigated in reference [22]. Moreover, resonant tunneling in different combinations, such as ENG-MNG-ENG, ENG-DPS-MNG, DPS-ENG-DPS, and ENG-DPS-ENG, has been extensively studied by Cojocaru [23]. In addition to this resonant tunneling in these bilayer and trilayer structures, there is another unusual feature, i.e., the wave transmission can be enhanced by increasing the loss from the constituent SNG media [24, 25]. Such unusual transmission has never been seen in the simple lossy materials like dielectric and metallic materials.

Referring to Fig. 1 and assuming the temporal part as $\exp(j\omega t)$ for all fields, the permittivity and permeability for the SNG media are expressible as

$$\varepsilon_1(\omega, \gamma_e) = \mathrm{Re}(\varepsilon_1) - j\mathrm{Im}(\varepsilon_1) = 1 - \frac{\omega_{ep}^2}{\omega^2 - j\gamma_e\omega}, \quad \mu_1 = a, \qquad (1)$$

with $\mathrm{Re}(\varepsilon_1) < 0$ and $a > 0$ for an ENG medium, and

$$\mu_2(\omega, \gamma_e) = \mathrm{Re}(\mu_2) - j\mathrm{Im}(\mu_2) = 1 - \frac{\omega_{mp}^2}{\omega^2 - j\gamma_m\omega}, \quad \varepsilon_2 = b, \qquad (2)$$

with $\mathrm{Re}(\mu_2) < 0$ and $b > 0$ for an MNG medium, respectively. In Eqs. (1) and (2), ω_{ep} and ω_{mp} are respectively the electric and

magnetic plasma frequencies. In addition, γ_e and γ_m are the electric and magnetic damping frequencies, respectively, and, in the meantime, they indicate the loss factors in the ENG and MNG media. It is apparent that the negative parameters, $\mathrm{Re}(\varepsilon_1)$ and $\mathrm{Re}(\mu_2)$, are frequency-dependent, whereas the parameters, a and b, are positive and static. In addition, based on Eq. (1), the refractive index of an ENG medium is

$$n_1(\omega, \gamma_e) = \sqrt{\varepsilon_1(\omega, \gamma_e)\,\mu_1} = \mathrm{Re}(n_1) - j\mathrm{Im}(n_1), \tag{3}$$

where

$$\begin{aligned} \mathrm{Re}(n_1) &= \sqrt{\frac{a}{2}}\left(|\varepsilon_1| + \mathrm{Re}(\varepsilon_1)\right)^{1/2}, \\ \mathrm{Im}(n_1) &= \sqrt{\frac{a}{2}}\left(|\varepsilon_1| - \mathrm{Re}(\varepsilon_1)\right)^{1/2}. \end{aligned} \tag{4}$$

Similarly, the refractive index of an MNG medium is given by

$$n_2(\omega, \gamma_m) = \sqrt{\mu_2(\omega, \gamma_m)\,\varepsilon_2} = \mathrm{Re}(n_2) - j\mathrm{Im}(n_2), \tag{5}$$

where

$$\begin{aligned} \mathrm{Re}(n_2) &= \sqrt{\frac{b}{2}}\left(|\mu_2| + \mathrm{Re}(\mu_2)\right)^{1/2}, \\ \mathrm{Im}(n_2) &= \sqrt{\frac{b}{2}}\left(|\mu_2| - \mathrm{Re}(\mu_2)\right)^{1/2}. \end{aligned} \tag{6}$$

The imaginary parts of n_1 and n_2, $\mathrm{Im}(n_1)$ and $\mathrm{Im}(n_2)$, are known as the extinction coefficients.

Previous studies on the wave properties of the ENG-MNG bilayer [19, 20, 24, 25] and of the SNG photonic crystals [15–18] are all done by assuming the static positive parameters, a and b, to be fixed as constants. In this paper, however, we shall show that, in this ENG-MNG bilayer structure, the resonant tunneling phenomenon will be strongly dependent on these two static positive parameters. It is found that electromagnetic resonant tunneling will happen when suitable values of a and b are chosen. The results suggest that the static positive material parameters may be playing important roles in the study of wave properties of layered structure containing the SNG media.

2. BASIC EQUATIONS

Let us start from the simple case of normal incidence. The resonant tunneling can be investigated by setting the reflection coefficient to be

zero, i.e., $r = 0$. Based on the transmission line theory (TLT), the reflection coefficient r can be calculated by way of the effective surface impedance $Z_{s,eff}\,(z=0)$ at plane boundary of $z = 0$, namely,

$$r = \frac{Z_{s,eff}\,(z=0) - Z_0}{Z_{s,eff}\,(z=0) + Z_0}, \tag{7}$$

where

$$Z_{s,eff}\,(z=0) = Z_1 \frac{Z\,(z=d_1) + Z_1 \tanh(\gamma_1 d_1)}{Z_1 + Z\,(z=d_1)\tanh(\gamma_1 d_1)}, \tag{8}$$

where

$$Z\,(z=d_1) = Z_2 \frac{Z_0 + Z_2 \tanh(\gamma_2 d_2)}{Z_2 + Z_0 \tanh(\gamma_2 d_2)}. \tag{9}$$

Here, $Z_0 = 377\,\Omega$ is the characteristic impedance of free space, as assumed in region 0 and 3, and $Z_1 = Z_0\sqrt{\mu_1/\varepsilon_1}$, $Z_2 = Z_0\sqrt{\mu_2/\varepsilon_2}$ are the characteristic impedances of the ENG and MNG layers, respectively. In addition, $\gamma_1 = jk_1 = j\,(\omega/c)\,n_1$ and $\gamma_2 = jk_2 = j\,(\omega/c)\,n_2$ are their corresponding propagation constants, where k_1 and k_2 are the associated wave numbers, and c is the speed of light in free space. The resonant tunneling occurs when the reflection coefficient is equal to zero, that is

$$Z_{s,eff}\,(z=0) = Z_0. \tag{10}$$

If both ENG and MNG layers are lossless, then Eq. (10), with the help of Eqs. (8) and (9) and some manipulations, leads to the following two conditions [19]

$$Z_1 = Z_2, \tag{11}$$

and

$$k_1 d_1 = k_2 d_2. \tag{12}$$

Eq. (11) is known as the condition of impedance match, while Eq. (12) is the phase match condition. With these two conditions, the ENG-MNG bilayer is referred to as the matched pair. Eqs. (11) and (12) reveal that the resonant tunneling relies on the static positive parameters, a and b. That is, the occurrence of tunneling depends on the suitable combinations of (a, b) when other material parameters are fixed.

In fact, the phase match condition, Eq. (12), is a direct consequence of the impedance match condition Eq. (11). This can be understood from the viewpoint of a one-dimensional SNG PC made by repeatedly stacking the resonant ENG-MNG bilayers. If the characteristic impedances of the constituent ENG and MNG layers are equal, as read in Eq. (11), then it is easy to have

$$k_1 \mu_2 = -k_2 \mu_1. \tag{13}$$

In a one-dimensional photonic crystal, the use of the Bloch theorem leads to the following characteristic equation that can be used to compute the band structure, [32]

$$\begin{aligned}\cos\left[K\left(d_1+d_2\right)\right] &= \cos\left(k_1 d_1\right)\cos\left(k_2 d_2\right) \\ &\quad -\frac{1}{2}\left(\frac{k_1\mu_2}{k_2\mu_1}+\frac{k_2\mu_1}{k_1\mu_2}\right)\sin\left(k_1 d_1\right)\sin\left(k_2 d_2\right), \quad (14)\end{aligned}$$

where K is the Bloch wave number, and k_1, k_2 are the wave numbers in the ENG and MNG layers, respectively. With Eq. (13), Eq. (14) can be reduced to

$$\cos\left[K\left(d_1+d_2\right)\right] = \cos\left(k_1 d_1 - k_2 d_2\right). \quad (15)$$

Since k_1 and k_2 are both purely imaginary, it can be seen from Eq. (15) that the condition for obtaining the real solution for K is only at $k_1 d_1 - k_2 d_2 = 0$, which is the phase match condition in Eq. (12). Conclusively, from TLT we have Eqs. (8) and (9), in which the complicated mathematical manipulations will be involved. The use of the photonic crystal, however, makes it easy to arrive at the match conditions from which the resonant tunneling attains in the matched pair.

Let us now consider the case of oblique incidence, in which there are two possible polarizations, the transversal electric (TE) and transversal magnetic (TM) waves, as illustrated in Fig. 1. In this case, the phase match condition for the resonant tunneling reads as

$$k_1 d_1 \cos\theta_1 = k_2 d_2 \cos\theta_2, \quad (16)$$

where the ray angles θ_1 and θ_2 are related to the Snell's law of refraction,

$$n_0 \sin\theta_0 = n_1 \sin\theta_1 = n_2 \sin\theta_2. \quad (17)$$

In addition, the impedance match condition becomes [33]

$$\frac{Z_1}{\cos\theta_1} = \frac{Z_2}{\cos\theta_2}, \quad (18)$$

for TE wave, and

$$Z_1 \cos\theta_1 = Z_2 \cos\theta_2, \quad (19)$$

for TM wave, respectively.

In our next analysis, the resonant tunneling will be investigated through the transmittance T calculated by making use of the transfer matrix method (TMM), with the result [34]

$$T = \left|\frac{1}{M_{11}}\right|^2, \quad (20)$$

where M_{11} is a matrix element of the total transfer matrix given by

$$\mathbf{M} = \begin{pmatrix} M_{11} & M_{12} \\ M_{21} & M_{22} \end{pmatrix} = \mathbf{D}_0^{-1} \left(\mathbf{D}_1 \mathbf{P}_1 \mathbf{D}_1^{-1} \mathbf{D}_2 \mathbf{P}_2 \mathbf{D}_2^{-1} \right) \mathbf{D}_3, \qquad (21)$$

where the dynamical matrix $\mathbf{D}_i$ (i = 0, 1, 2, and 3) and the translational matrix $\mathbf{P}_i$ (i = 1 and 2) in Eq. (21) can be found in Ref. [32].

3. NUMERICAL RESULTS AND DISCUSSION

Before we present the numerical results for the transmittance, we first illustrate the frequency range for the SNG materials. The plasma frequencies for the ENG and MNG media are taken to be $\omega_{ep}(2\pi f_{ep}) = 10\,\text{GHz}$ and $\omega_{mp}(2\pi f_{mp}) = 17.3\,\text{GHz}$, respectively [24]. According to Eqs. (1) and (2) with no loss ($\gamma_e = \gamma_m = 0$), we can plot the frequency-dependent $\text{Re}(\varepsilon_1)$ and $\text{Re}(\mu_2)$, as shown in Fig. 2. It can be seen from Fig. 2 that the valid linear frequency range is from 0.4 GHz to 1.2 GHz, over which both $\text{Re}(\varepsilon_1)$ and $\text{Re}(\mu_2)$ are negative, and the absolute values in $\text{Re}(\mu_2)$ are larger than $\text{Re}(\varepsilon_1)$. This frequency range will be used to calculate the transmittance for the ENG-MNG bilayer.

3.1. Lossless Bilayer with Equal-thicknesses Layers

Let us first consider the lossless bilayer with equal-thicknesses layers, i.e., $\gamma_e = \gamma_m = 0$, and $d_1 = d_2 = d$. Fig. 3 depicts the normal-incidence transmittance versus frequency for various values of $a = \mu_1 = 0.1$, 1,

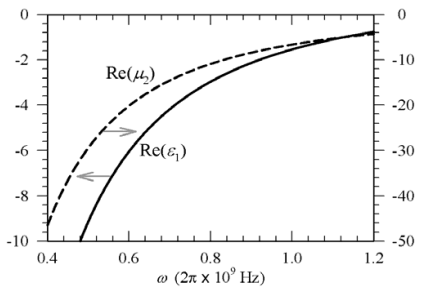

Figure 2. The frequency range for both negative $\text{Re}(\varepsilon_1)$ and $\text{Re}(\mu_2)$. Here, $\gamma_e = \gamma_m = 0$ is used.

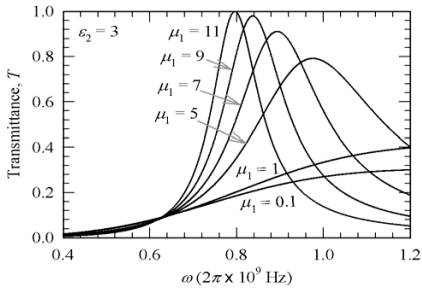

Figure 3. The frequency dependence of transmittance in the lossless ENG-MNG bilayer at different values of μ_1 for a fixed $\varepsilon_2 = 3$. Here $d_1 = d_2 = 15\,\text{mm}$.

5, 7, 9, and 11 at a fixed static $b = \varepsilon_2 = 3$ and $d = 15\,\text{mm}$. It can be seen that the resonant tunneling can happen at a large value of a. A salient tunneling peak starts to appear when a is larger than or equal to five. The peak frequency is shifted to the lower frequency and the peak shape becomes narrow as a increases. At $a = 9$, the peak height arrives at $T = 0.979$. As shown in the figure, a complete resonant tunneling, $T = 1$, will occur at $a = 11$ with a resonant frequency of $\omega_{res} = 0.79 \times 2\pi \times 10^9\,\text{Hz}$. That is, a set of $a = 11$ and $b = 3$ can yield the desired complete resonant tunneling. Such specific values of static positive parameters can be understood by the impedance match and phase match conditions, Eqs. (11) and (12). Using these two conditions with $d_1 = d_2$, the values of a and b can be determined by the following relations, namely

$$\mu_1 = a = |\mu_2|\,, \quad \varepsilon_2 = b = |\varepsilon_1|\,. \tag{22}$$

It is of interest to note that the positive parameter a (the permeability) of the ENG medium is equal to the magnitude of the negative parameter μ_2 (the permeability) of the MNG medium, and the positive parameter b (the permittivity) of the MNG medium is equal to the magnitude of the negative parameter ε_1 (the permittivity) of the ENG medium. With this resonant frequency of $\omega_{res} = 0.79 \times 2\pi \times 10^9\,\text{Hz}$, simple calculations on Eqs. (1) and (2) give rise to $|\varepsilon_1(\omega_{res}, 0)| = 3$, and $|\mu_2(\omega_{res}, 0)| = 11$, which are in good agreement with Fig. 3. Conversely, one can first assign the resonant frequency in the interested frequency range and then, with this resonant frequency, the static positive parameters can be determined from Eq. (22). Thus, Eq. (22) plays a useful and important role in determining the static material parameter in order to achieve the resonant tunneling. As for the field distribution in the bilayer structure at resonant tunneling, we mention the reference [19].

In addition, based on the above discussion, we find that at the set of $a = 11$ and $b = 3$ the resonant frequency ω_{res} has nothing to do with the thickness $d_1 = d_2 = d$, that is, it remains unchanged no matter what d is taken. This independence has been illustrated in Fig. 4, in which the resonant frequency is the same for all different values of d. The only influence of d is to cause the resonant peak to be much narrower when d increases. At $d = 30\,\text{mm}$, an extremely narrow resonant peak is obtained. If this bilayer is utilized to act as a narrowband transmission filter, then the thicker bilayer will be preferable to reaching this goal.

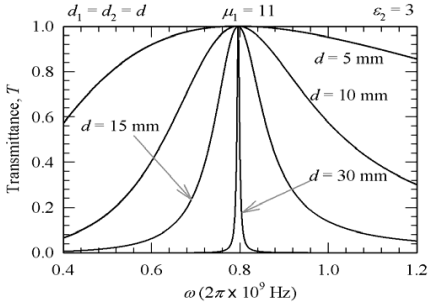

Figure 4. The frequency dependence of transmittance in the lossless ENG-MNG bilayer at different values of d for a fixed $\mu_1 = 11$ and $\varepsilon_2 = 3$.

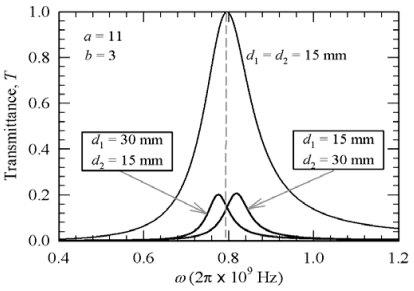

Figure 5. The effect of unequal-thicknesses layers at $\mu_1 = a = 11$ and $\varepsilon_2 = b = 3$. The resonant frequency moves to the right for $d_1 < d_2$, while it moves to the left for $d_1 > d_2$.

3.2. Lossless Bilayer with Unequal-thicknesses Layers

In the case of unequal-thicknesses layers, $d_1 \neq d_2$, the resonant tunneling at $a = 11$ and $b = 3$ will be strongly suppressed. This is depicted in Fig. 5, in which the resonant frequency will slightly be shifted to the right or left, depending on $d_1 < d_2$ or $d_1 > d_2$. The pronounced suppression in the peak height also reveals that the values of $a = 11$ and $b = 3$ are no longer valid for the matched pair in this case.

In case $d_1 \neq d_2$ the expressions for determining the static positive parameters a and b in Eq. (22) must be modified as follows:

$$\mu_1 = a = \frac{d_2}{d_1}\left|\mu_2\right|, \quad \varepsilon_2 = b = \frac{d_1}{d_2}\left|\varepsilon_1\right|. \tag{23}$$

Eq. (23), which can be easily obtained from the impedance and phase match conditions, provides the guidance of how to select the static positive parameters at a desired resonant frequency. For instance, as in Fig. 4, we fix the resonant frequency at $\omega_{res} = 0.79 \times 2\pi \times 10^9$ Hz, then $|\varepsilon_1(\omega_{res}, 0)| = 3$ and $|\mu_2(\omega_{res}, 0)| = 11$. Thus, if we take $d_1 = 22$ (33, 44) mm and $d_2 = 6$ (9, 12) mm, then a complete resonance will appear at a fixed set of $a = 3$ and $b = 11$ according to Eq. (23). This complete resonance is evidently shown in Fig. 6. In addition to fixing the resonant frequency at different sets of d_1 and d_2, it is seen that the peak shape becomes narrow at a larger total length of $d_1 + d_2$. This narrowing effect is also seen in the case of equal-thicknesses layers, as depicted in Fig. 4.

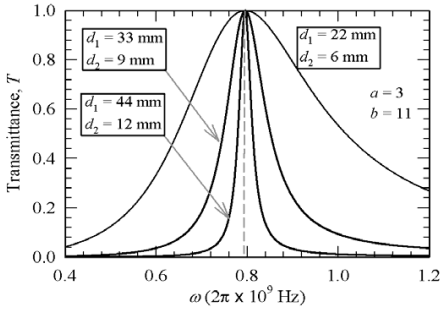

Figure 6. The effect of unequal-thicknesses layers at $\mu_1 = 3$ and $\varepsilon_2 = 11$. The resonant frequency remains fixed for three different combinations of d_1 and d_2.

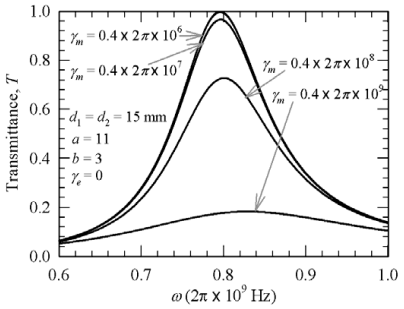

Figure 7. The frequency dependence of transmittance for the ENG-MNG bilayer at different values of the magnetic loss. Here, $a = 11$, $b = 3$, and $\gamma_e = 0$.

3.3. Effects of Losses on Resonant Tunneling

To investigate the effects of losses on the resonant tunneling, let us limit to the case of equal-thicknesses layers with $a = 11$ and $b = 3$. In Fig. 7, we plot the transmittance for different magnetic losses at zero electric loss $\gamma_e = 0$ and $d_1 = d_2 = 15\,\text{mm}$. Like in the usual two-layer dielectric Fabry-Perot resonator, the inclusion of loss strongly affects the resonant peak height. Strong suppression will be seen at a higher loss factor. The peak frequency, however, remains nearly unchanged when the loss is below the moderate value.

The similar depression in the resonant peak height is also present when we consider the electric loss or both losses. The nearly no shift in the resonant frequency in the low-loss case allows us to safely use Eqs. (22) and (23) to estimate the static positive parameters by first setting the loss to zero. Strictly speaking on the results in Fig. 7, losses change the resonance peak frequency somewhat as shown in Fig. 16 in the reference [35].

3.4. Investigation of Polarization-dependent Resonant Tunneling

Let us now examine how the polarization of incident wave affects the resonant tunneling in the SNG bilayer. In Figs. 8 and 9, we have respectively plot the TE- and TM-wave transmittance for the distinct angles of incidence. Here, both ENG and MNG media are lossless, and the static positive parameters, $\mu_1 = a = 9$ and $\varepsilon_2 = b = 3$ are used.

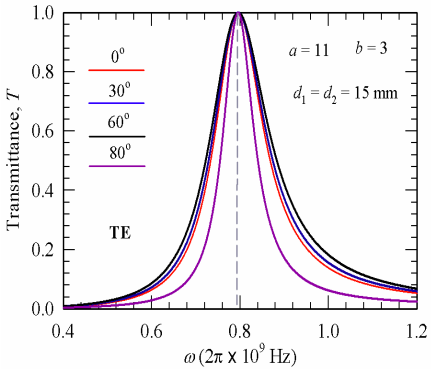

Figure 8. The frequency dependence of TE-wave transmittance in the lossless ENG-MNG bilayer at different angles of incidence.

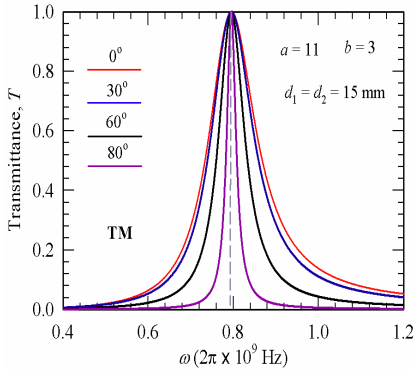

Figure 9. The frequency dependence of TM-wave transmittance in the lossless ENG-MNG bilayer at different angles of incidence.

The transmittance spectra near the resonant point for TE and TM waves are plotted in Figs. 8 and 9, respectively. It is of interest to see that the resonant frequency is independent of the angle of incidence for both polarizations. This insensitivity is similar to the SNG gap existing in the one-dimensional SNG photonic crystal made of ENG-MNG bilayers [15]. The role played by the incident angle is to narrow the resonant shape, especially in the TM wave. This narrowing feature as a function of angle of incidence is, however, not so strong in the TE wave.

In view of the filter design, the narrow transmittance spectrum indicates that the ENG-MNG bilayer can be used to function as a narrowband transmission filter. That means, in the TM wave, the increase in the angle of incidence can be used to significantly enhance the quality factor. Based on Figs. 8 and 9, we conclude that a narrowband transmission filter can be achieved by choosing the TM wave instead of the TE wave.

3.5. Potential Application: A Multi-resonance Filter

Let us finally discuss the potential application of the resonant ENG-MNG bilayer, i.e., a multichanneled transmission filter can be achieved by cascading distinct bilayers of different resonant frequencies. A cascaded structure will have multiple resonant peaks because it has the collected resonant modes [36]. For instance, we can obtain a filter

with double resonant peaks in a two-bilayer structure such as (ENG-MNG)$_1$(ENG-MNG)$_2$. By selecting two different sets of (a, b) we can arbitrarily design two different resonant frequencies, ω_1 and ω_2, for (ENG-MNG)$_1$ and (ENG-MNG)$_2$, respectively. Thus, the cascaded structure (ENG-MNG)$_1$(ENG-MNG)$_2$ will have two resonant peaks at ω_1 and ω_2 and consequently two-channel filter is achievable. Similarly, by cascading more bilayers with distinct resonant frequencies, we shall arrive at a multichanneled filter. Such a multichanneled filter is structurally different from that designed by using the photonic crystal with the photonic-quantum-well defect [37].

4. CONCLUSION

The dependence of electromagnetic resonant tunneling on the two static positive material parameters, a (the permeability of ENG medium) and b (the permittivity of MNG medium), in the ENG-MNG bilayer has been systematically investigated in this work. Since the complete resonant tunneling occurs at the matched pair, we find that the frequency for the resonant tunneling is strongly related to the suitable values of a and b. We have studied the resonant tunneling in two possible cases of the equal-thicknesses and unequal-thicknesses bilayers. In the lossless equal-thicknesses SNG bilayer, we find the relations of how to determine these two static positive parameters if the desired resonant frequency is assigned in advance. These relations are then extended to the case of the unequal-thicknesses case. We next study the effects of losses coming from the ENG and MNG media. It is found that the resonant frequency is nearly unchanged in the presence of the low-loss and moderate loss cases. Finally, the frequency of the resonant tunneling is independent of the angle of incidence for both the TE and TM waves. In TM-polarization, the peak shape is strongly narrowed as the angle increases. This narrowing feature leads to an enhancement in the quality factor, which is preferable to the design of a narrowband transmission filter based on the SNG bilayer.

ACKNOWLEDGMENT

C.-J. Wu acknowledges the financial support from the National Science Council of the Republic of China (Taiwan) under Contract No. NSC-97-2112-M-003-013-MY3.

REFERENCES

1. Veselago, V. G., "The electrodynamics of substances with simultaneously negative values of ε and μ," *Sov. Phys. Usp.*, Vol. 10, 509–514, 1968.
2. Smith, D. R., W. J. Padilla, D. C. Vier, S. C. Nemat-Nasser, and S. Schultz, "Composite medium with simultaneously negative permeability and permittivity," *Phys. Rev. Lett.*, Vol. 84, 4184–4187, 2000.
3. Shelby, R. A., D. R. Smith, and S. Schultz, "Experimental verification of a negative index of refraction," *Science*, Vol. 292, 77–97, 2001.
4. Liu, Y., X. Chen, and K. Huang, "A novel planar printed array antenna with SRR slots," *Journal of Electromagnetic Waves and Applications*, Vol. 24, No. 16, 2155–2164, 2010.
5. Hsu, H. T., T. W. Chang, T.-J. Yang, B.-H. Chu, and C.-J. Wu, "Analysis of wave properties in photonic crystal narrowband filters with left-handed defect," *Journal of Electromagnetic Waves and Applications*, Vol. 24, No. 16, 2285–2298, 2010.
6. Wu, Z., B. Q. Zeng, and S. Zhong, "A double-layer chiral metamaterial with negative index," *Journal of Electromagnetic Waves and Applications*, Vol. 24, No. 7, 983–992, 2010.
7. Sabah, C., "Novel, dual band, single and double negative metamaterials: nonconcentric delta loop resonators," *Progress In Electromagnetics Research B*, Vol. 25, 225–239, 2010.
8. Sabah, C., "Tunable metamaterial design composed of triangular split ring resonator and wire strip for s- and c-microwave bands," *Progress In Electromagnetics Research B*, Vol. 22, 341–357, 2010.
9. Essadqui, A., J. Ben-Ali, D. Bria, B. Djafari-Rouhani, and A. Nougaoui, "Photonic band structure of 1D periodic composite system with left handed and right handed materials by green function approach," *Progress In Electromagnetics Research B*, Vol. 23, 229–249, 2010.
10. Al-Naib, I. A. I., C. Jansen, and M. Koch, "Single metal layer CPW metamaterial bandpass filter," *Progress In Electromagnetics Research Letters*, Vol. 17, 153–161, 2010.
11. Gu, C., S. Qu, Z. Pei, H. Zhou, J. Wang, B.-Q. Lin, Z. Xu, P. Bai, and W.-D. Peng, "A wide-band, polarization-insensitive and wide-angle terahertz metamaterial absorber," *Progress In Electromagnetics Research Letters*, Vol. 17, 171–179, 2010.
12. Rahimi, H., "Backward tamm states in 1D single-negative metamaterial photonic crystals," *Progress In Electromagnetics*

Research Letters, Vol. 13, 149–159, 2010.

13. Gennarelli, G. and G. Riccio, "Diffraction by a lossy double-negative metamaterial layer: A uniform asymptotic solution," *Progress In Electromagnetics Research Letters*, Vol. 13, 173–180, 2010.
14. Fredkin, D. R. and A. Ron, "Effective left-handed (negative index) composite material," *Appl. Phys. Lett.*, Vol. 81, 1753–1755, 2002.
15. Wang, L. G., H. Chen, and S. Y. Zhou, "Omnidirectional gap and defect mode of one-dimensional photonic crystals with single-negative materials," *Phys. Rev. B*, Vol. 70, 245102, 2004.
16. Yeh, D.-W. and C.-J. Wu, "Analysis of photonic band structure in a one-dimensional photonic crystal containing single-negative material," *Optics Express*, Vol. 17, 16666–16680, 2009.
17. Yeh, D.-W. and C.-J. Wu, "Thickness-dependent photonic bandgap in a one-dimensional single-negative photonic crystal," *J. Opt. Soc. Am. B*, Vol. 26, 1506–1510, 2009.
18. Luo, Z., Z. Tang, H. Luo, and S. Wen, "Polarization-independent low-pass spatial filters based on one-dimensional photonic crystals containing negative-index materials," *App. Phys. B*, Vol. 94, 641–646, 2009.
19. Alu, A. and N. Engheta, "Pairing an epsilon-negative slab with a mu-negative slab: Resonance, tunneling and transparency," *IEEE Trans. Antenna Propagation*, Vol. 51, 2558–2571, 2003.
20. Ding, Y., Y. Li, H. Jiang, and H. Chen, "Electromagnetic tunneling in nonconjugated epsilon-negative and mu-negative metamaterial pair," *PIERS Online*, Vol. 6, No. 2, 109–112, 2010.
21. Feng, T., Y. Li, H. Jiang, Y. Sun, L. He, H. Li, Y. Zhang, Y. Shi, and H. Chen, "Electromagnetic tunneling in a sandwich structure containing single negative media," *Phys. Rev. E*, Vol. 79, 026601, 2009.
22. Castaldi, G., I. Gallina, V. Galdi, A. Alu, and N. Engheta, "Electromagnetic tunneling through a single-negative slab paired with a double-positive bilayer," *Phys. Rev. B*, Vol. 83, 081105(R), 2011.
23. Cojocaru, E., "Electromagnetic tunneling in lossless trilayer stacks containing single-negative metamaterials," *Progress In Electromagnetics Research*, Vol. 113, 227–249, 2011.
24. Dong, L., G. Du, H. Jiang, H. Chen, and Y. Shi, "Transmission properties of lossy single-negative materials," *J. Opt. Soc. Am. B*, Vol. 26, 1091–1096, 2009.
25. Lin, W.-H., C.-J. Wu, and S.-J. Chang, "Analysis of angle-

dependent unusual transmission in lossy single-negative (SNG) materials," *Solid State Comm.*, Vol. 150, 1729–1732, 2010.

26. Lin, W.-H., C.-J. Wu, and S.-J. Chang, "Angular dependence of wave reflection in a lossy single-negative bilayer," *Progress In Electromagnetics Research*, Vol. 107, 253–267, 2010.
27. Smolyakov, A. I., E. A. Fourkal, S. I. Krasheninnikov, and N. Sternberg, "Resonant modes and resonant transmission in multi-layer structures," *Progress In Electromagnetics Research*, Vol. 107, 293–314, 2010.
28. Bucinskas, J., L. Nickelson, and V. Shugurovas, "Microwave scattering and absorption by a multilayered lossy metamaterial glass cylinder," *Progress In Electromagnetics Research*, Vol. 105, 103–118, 2010.
29. Rahimi, H., A. Namdar, S. Roshan Entezar, and H. Tajalli, "Photonic transmission spectra in one-dimensional fibonacci multilayer structures containing single-negative metamaterials," *Progress In Electromagnetics Research*, Vol. 102, 15–30, 2010.
30. Sabah, C. and S. Uckun, "Multilayer system of lorentz/drude type metamaterials with dielectric slabs and its application to electromagnetic filters," *Progress In Electromagnetics Research*, Vol. 91, 349–364, 2009.
31. Li, Y., Q. Zhu, Y. Yan, S.-J. Xu, and B. Zhou, "Design of a $1 * 20$ series feed network with composite right/left-handed transmission line," *Progress In Electromagnetics Research*, Vol. 89, 311–324, 2009.
32. Canto, J. R., S. A. Matos, C. R. Paiva, and A. M. Barbosa, "Effects of losses in a layered structure containing DPS and DNG media," *PIERS Online*, Vol. 4, No. 5, 546–550, 2008.
33. Orfanidis, S. J., *Electromagnetic Waves and Antennas*, Chapter 7, Rutger University, 2008, www.ece.rutgers.edu/∼orfanidi/ewa.
34. Yeh, P., *Optical Waves in Layered Media*, John Wiley & Sons, Singapore, 1991.
35. Jung, K.-Y. and F. L. Teixeira, "Photonic crystals with a degenerate band edge: Field enhancement effects and sensitivity analysis," *Phys. Rev. B*, Vol. 77, 125108, 2008.
36. Wang, L., Z. Shen, B. Fan, and Z. Wang, "High transmittance of connected resonant modes," *Optics Comm.*, Vol. 283, 2155–2159, 2010.
37. Qiao, F., C. Zhang, J. Wan, and J. Zi, "Photonic quantum-well structures: multiple channeled filtering phenomena," *Appl. Phys. Lett.*, Vol. 77, No. 23, 3698–3701, 2000.